

Undertaker, a *Drosophila* Junctophilin, Links Draper-Mediated Phagocytosis and Calcium Homeostasis

Leigh Cuttell,^{1,2,3} Andrew Vaughan,^{1,2} Elizabeth Silva,¹ Claire J. Escaron,^{1,4} Mark Lavine,^{1,5} Emeline Van Goethem,^{1,6} Jean-Pierre Eid,¹ Magali Quirin,^{1,7} and Nathalie C. Franc^{1,*}

¹Medical Research Council Cell Biology Unit, MRC Laboratory for Molecular Cell Biology and Cell and Developmental Biology Department, University College London, Gower Street, London WC1E 6BT, UK

²These authors contributed equally to this work

³Present address: School of Veterinary Science, University of Queensland, St Lucia, QLD 4072, Australia

⁴Present address: Division of Cell and Molecular Biology, Centre for Molecular Microbiology and Infection, Imperial College London, London SW7 2AZ, UK

⁵Present address: Department of Microbiology, Molecular Biology, and Biochemistry, University of Idaho, Moscow, ID 83844-3052, USA

⁶Present address: Institut de Pharmacologie et Biologie Structurale, CNRS UMR 5089, 31077 Toulouse Cedex, France

⁷Present address: Laboratory of Developmental Biology, UMR 7009 CNRS-UPMC, Observatoire Océanologique, 06230 Villefranche-sur-Mer, France

*Correspondence: n.franc@ucl.ac.uk

DOI 10.1016/j.cell.2008.08.033

SUMMARY

Phagocytosis is important during development and in the immune response for the removal of apoptotic cells and pathogens, yet its molecular mechanisms are poorly understood. In *Caenorhabditis elegans*, the CED2/5/10/12 pathway regulates actin during phagocytosis of apoptotic cells, whereas the role of the CED1/6/7 pathway in phagocytosis is unclear. We report that Undertaker (UTA), a *Drosophila* Junctophilin protein, is required for Draper (CED-1 homolog)-mediated phagocytosis. Junctophilins couple Ca²⁺ channels at the plasma membrane to those of the endoplasmic reticulum (ER), the Ryanodine receptors. We place Draper, its adaptor drCed-6, UTA, the Ryanodine receptor Rya-r44F, the ER Ca²⁺ sensor dSTIM, and the Ca²⁺-release-activated Ca²⁺ channel dOrai in the same pathway that promotes calcium homeostasis and phagocytosis. Thus, our results implicate a Junctophilin in phagocytosis and link Draper-mediated phagocytosis to Ca²⁺ homeostasis, highlighting a previously uncharacterized role for the CED1/6/7 pathway.

INTRODUCTION

Phagocytosis is a crucial process during development and in innate immunity of all multicellular organisms. It allows for rapid engulfment of dying cells and pathogens by specialized phagocytes, such as macrophages and neutrophils in mammals (Aderem and Underhill, 1999). Phagocytosis is also an essential function of dendritic cells that present processed antigens to lymphocytes, thus linking innate and adaptive immunity (Lee and Iwasaki, 2007).

In *Caenorhabditis elegans*, the death genes *ced-2*, *5*, *10*, and *12* activate the small GTPase CED-10 that triggers actin cytoskeleton rearrangement during phagocytosis; the parallel CED1/6/7 pathway also converges on CED-10, but its precise role in phagocytosis remains elusive (Mangahas and Zhou, 2005).

During *Drosophila* embryogenesis, two macrophage receptors, Croquemort (CRQ), a CD36 homolog (Franc et al., 1999), and Draper (DRPR), a CED-1 homolog (Manaka et al., 2004), play a role in apoptotic cell clearance, much like their counterparts in mammals or *C. elegans*. The *Drosophila* homolog of CED-6, Dmel/Ced-6 (hereafter called drCed-6), and DRPR are also required in glial cells for axon pruning and the engulfment of degenerating neurons (Awasaki et al., 2006; MacDonald et al., 2006).

In a deficiency screen, we characterized a mutant in which embryonic macrophages poorly engulfed apoptotic cells. In an RNAi screen using S2 cells, we identified *undertaker/retinophilin* (*uta*) as being responsible for this phenotype. *uta* encodes a membrane occupational and recognition nexus (MORN) repeat-containing protein with homology to mammalian Junctophilins (JPs). JPs form junctional complexes between the plasma membrane (PM) and the endoplasmic/sarcoplasmic reticulum (ER/SR) Ca²⁺ storage compartment (Takeshima et al., 2000). These complexes allow for crosstalk between Ca²⁺ channels at the PM and the ER/SR Ca²⁺ channels, or Ryanodine receptors (RyRs), thus regulating Ca²⁺ homeostasis and functions of excitable cells (Takeshima et al., 2000). Although a role for Ca²⁺ in phagocytosis of various particles by mammalian phagocytes has been previously described, the molecular mechanisms underlying Ca²⁺ fluxes associated with these events are not known (Dewitt and Hallett, 2002; Rubartelli et al., 1997; Tejle et al., 2002).

We report that, as for UTA, the *Drosophila* Ryanodine receptor, Rya-r44F (Xu et al., 2000), plays a role in phagocytosis of apoptotic cells in vivo. We also found a requirement in phagocytosis for

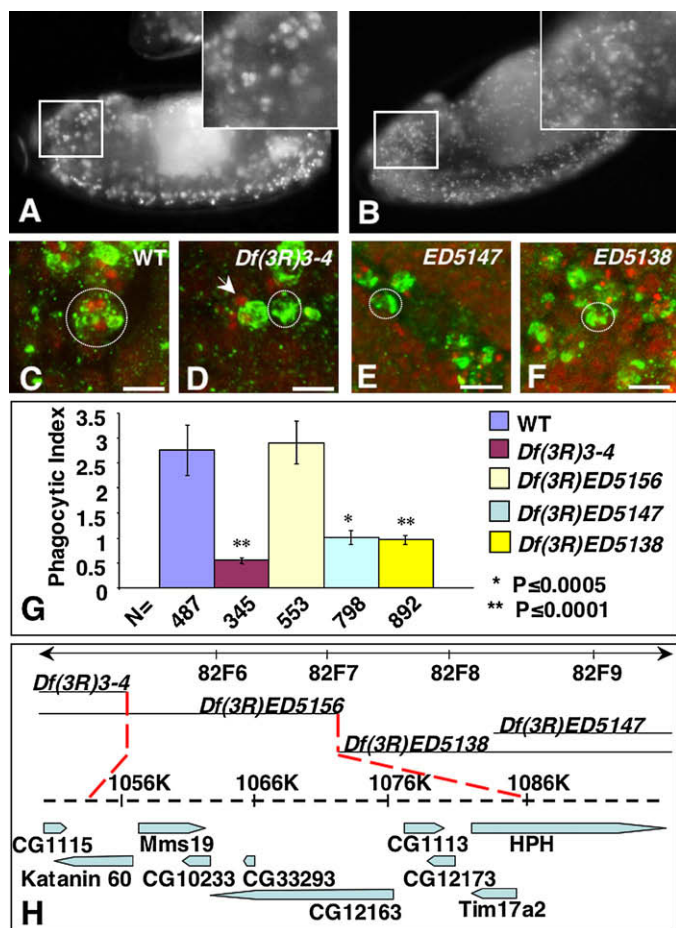


Figure 1. Phagocytosis of Apoptotic Cell Defect in *Df(3R)3-4* Homozygous Embryos

(A and B) Wild-type (A) and *Df(3R)3-4* homozygous mutant (B) AO-stained stage 13 embryos (anterior to the left, dorsal side to the top). Insets show higher-magnified views of AO-stained corpses.

(C–F) Macrophages of stage 13 embryos stained with CRQ Ab (green) and 7-AAD (red) that brightly stain apoptotic corpses in wild-type (C), *Df(3R)3-4* (D), *Df(3R)ED5147* (E), and *Df(3R)ED5138* (F) homozygous embryos. The arrow in (D) points to an apoptotic cell seen in close proximity to the mutant macrophage that is not engulfed, as it is not fully surrounded by CRQ staining. Circles indicate single macrophages. Scale bars represent 10 μ m.

(G) A graph of the corresponding PIs \pm SD. N, number of macrophages scored. p values are indicated using asterisks.

(H) A schematic of the 82F region of the genome indicating the breakpoints of the deficiencies.

embryos for Croquemort (CRQ), a macrophage marker, and with 7-amino actinomycin D (7-AAD) to label apoptotic cells (Silva et al., 2007). Phagocytosis phenotypes were quantified by averaging the number of engulfed corpses per macrophage, which are reported as phagocytic indices (PI). Wild-type macrophages were large and efficiently engulfed apoptotic cells, with a PI of 2.73 ± 0.5 (Figure 1C; see Figures S1A, S1E, and S1H available online). Homozygous *Df(3R)3-4* macrophages poorly engulfed apoptotic cells, with a PI of 0.55 ± 0.06 (Figure 1G), and were small in size (Figure 1D). They migrated to the sites of apoptosis (Figure S1B), occasionally engulfed one corpse (Figure 1D), and, as in wild-type, *Df(3R)3-4* macrophages endocytosed injected acetylated low-density lipoproteins, a scavenger receptor ligand, thereby attesting to their differentiated and functional state (Figures S1C and S1D).

We mapped the molecular breakpoints of *Df(3R)3-4* between *CG10299* (*Katanin 60*) and *CG12005/Mms19*, and within *Hph* (Figure 1H). We next examined the phenotypes of the overlapping deletions *Df(3R)ED5138*, *Df(3R)ED5147*, and *Df(3R)ED5156* for which breakpoints have been precisely mapped (Ryder et al., 2004) (Figure 1H). *Df(3R)ED5156* homozygous macrophages were wild-type for phagocytosis of apoptotic corpses, with a PI of 2.90 ± 0.43 versus 2.73 ± 0.5 in wild-type ($p = 0.57$) (Figure 1G; Figures S1F and S1I). *Df(3R)ED5147* and *Df(3R)ED5138* homozygous macrophages poorly engulfed apoptotic corpses, with PIs of 0.99 ± 0.15 and 0.95 ± 0.09 , respectively, despite elevated levels of apoptosis in the deficient embryos (Figures 1E–1G and S1G). Thus, we defined the region of interest to eight genes between *CG10229/Katanin 60* and *CG31543/dHPH* (Figure 1H).

store-operated Ca^{2+} entry (SOCE) via dSTIM, a Ca^{2+} sensor of the ER/SR lumen (Roos et al., 2005), and CRACM1/dOrai, a Ca^{2+} -release-activated Ca^{2+} channel (CRAC) (Feske et al., 2006; Vig et al., 2006). We show that *uta* and *rya-r44F* genetically interact with *drced-6* and *drpr*, and that *uta*, *drced6*, and *drpr* are required for SOCE in S2 cells. Thus, these genes act in the same pathway that plays a general role in phagocytosis, as *uta*, *dstim*, *dorai*, *drced-6*, and *drpr* are also required for efficient phagocytosis of bacteria. Our results provide a link between SOCE and phagocytosis, imply that UTA plays a similar role in macrophages to that of JPs in excitable cells, and shed light on a role for the CED1/6/7 pathway in Ca^{2+} homeostasis during phagocytosis.

RESULTS

Df(3R)3-4, a Deficiency Mutant, Has Reduced Phagocytosis of Apoptotic Cells

In a deficiency screen using acridine orange (AO) to identify mutants for apoptotic cell engulfment in the *Drosophila* embryo (Silva et al., 2007), we found that embryos homozygous for *Df(3R)3-4*, a large deletion of the 82F genomic region, lacked clustering of AO-stained apoptotic corpses (compare Figures 1A and 1B), indicating that macrophages may be phagocytosis defective. To characterize the deficiency phenotype, we stained

undertaker/retinophilin Is Required for Efficient Engulfment of Apoptotic Cells

To assess the potential role for each of the eight candidate genes in apoptotic cell clearance, we developed a phagocytosis assay in cultured Schneider S2 cells. These are *Drosophila* embryo-derived cells with macrophage-like properties that can engulf apoptotic cells, Gram-negative (*Escherichia coli*) and -positive bacteria (*Staphylococcus aureus*), and small fungi, such as *Candida silvatica* (Ramet et al., 2001). In this

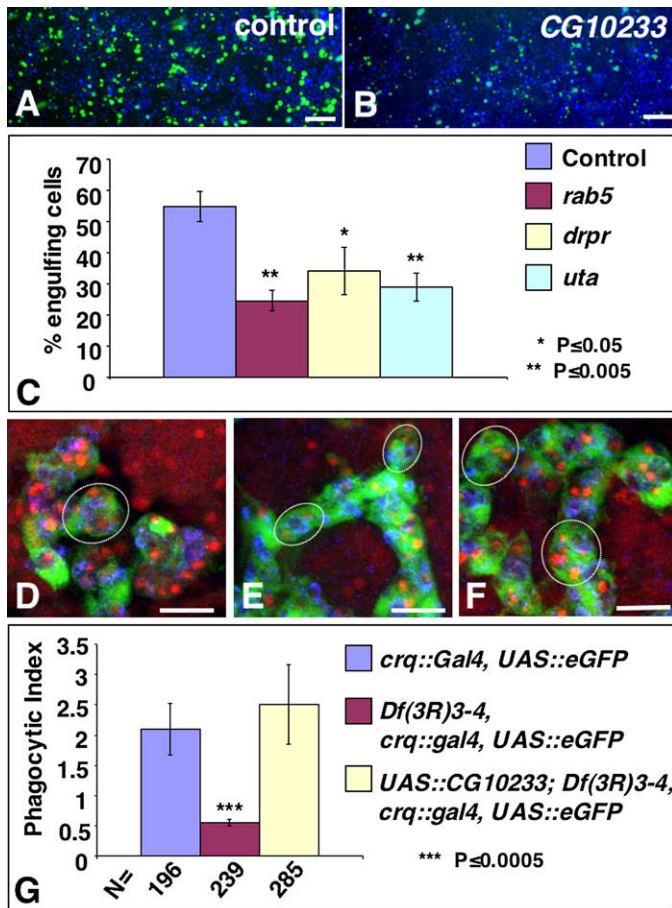


Figure 2. Requirement for *CG10233/undertaker* in Phagocytosis of Apoptotic Cells

(A and B) Phagocytosis of apoptotic cells by mock- (A) or *uta* RNAi-treated (B) S2 cells. Scale bars represent 200 μ m.

(C) A graph summarizing the quantification of these assays with *rab5* RNAi-treated S2 cells as a control. Bars represent the mean percentage of engulfing cells \pm standard errors from the mean (SEM) of three independent experiments with duplicated wells.

(D–F) Merged confocal images of *yw; +; crq::Gal4, UAS::eGFP* (wild-type reference) (D), *yw; +; Df(3R)3-4, crq::Gal4, UAS::eGFP* (mutant reference) (E), and *yw: UAS::CG10233; Df(3R)3-4, crq::Gal4, UAS::eGFP* homozygous macrophages (rescue) (F). Apoptotic cells are stained with 7-AAD (red), GFP-expressing macrophages appear green, and CRQ Ab is in blue. Scale bars represent 10 μ m.

(G) A graph of the mean PIs \pm SD of these macrophages.

likely candidate gene responsible for the deficiency phenotype.

To address whether *CG10233* is required for phagocytosis in vivo, we used a *crq::gal4* driver to express a *UAS::CG10233* transgene, along with *UAS::eGFP*, in *Df(3R)3-4* mutant macrophages (Figure 2F) and compared these macrophages' phenotype to that of embryos where the *UAS::CG10233* transgene was absent (Figure 2E). The reexpression of *CG10233* in *Df(3R)3-4* mutant macrophages rescued their ability to efficiently engulf apoptotic cells (Figures 2F and 2G), with a PI of 2.50 ± 0.66 versus 0.55 ± 0.06 in the mutant (Figures 2E and 2G) and 2.09 ± 0.43 in control *crq::Gal4, UAS::eGFP* macrophages (Figures 2D and 2G; $p = 0.33$). Thus, *CG10233* is required in macrophages to promote apoptotic cell clearance. We renamed *CG10233* as *undertaker* (*uta*), as its mutant phenotype is reminiscent of that of *crq* and *pallbearer* (*pall*) deletion mutants (Franc et al., 1999; Silva et al., 2007). While our work was in progress, *CG10233* was also named *retinophilin*, as it is expressed in the fly retina (Mecklenburg, 2007).

uta* Behaves as a JP and Genetically Interacts with the Ryanodine Receptor Gene *rya-r44F

uta encodes two JP-related protein isoforms with two and four MORN repeats (Figure 3A) (Mecklenburg, 2007). To assess whether UTA may form similar junctional complexes between PM and ER to those formed by JPs in mammalian excitable cells, we stained S2 cells or embryonic macrophages using a Retinophilin/UTA Ab (Mecklenburg, 2007), while marking the PM using an Ab against the Na^+/K^+ ATPase α subunit (Lebovitz et al., 1989) (Figures 3B–3D), or the ER using Abs against PDI (Burlak et al., 2006) or KDEL (Pinto et al., 2006) (Figures 3I and 3J). We observed some colocalization between UTA and the Na^+/K^+ ATPase α subunit in puncta at the PM ruffling of S2 cells (Figure 3D and inset), as well as at the site of apoptotic cell engulfment (arrow in Figure 3D). There was also some colocalization between CRQ and UTA on embryonic macrophages, in both small intracellular vesicles and large vesicles, which are likely to contain apoptotic corpses, arguing that UTA may be present on the phagosome (Figures 3E–3G; inset in Figure 3G). We confirmed this colocalization of CRQ and UTA on phagosomes containing apoptotic cells in S2 cells (Figure 3H). As

assay, S2 cells were incubated with an excess of FITC-labeled fixed apoptotic S2 cells to allow for engulfment, and then counterstained with Cell Tracker Blue CMAC (CTB), a fluorescent live-cell dye. The fluorescence of bound or free apoptotic cells was quenched using the previously characterized trypan blue method (Ramet et al., 2001), so that the only remaining FITC detected was that of fully engulfed apoptotic cells (Figure S2A). As expected, trypan blue quenched the fluorescence of all apoptotic cells when the assay was carried out at 4°C, which is nonpermissive to particle engulfment (Figure S2B). We validated the assay by subjecting it to conditions that positively or negatively affect phagocytosis (see Supplemental Data).

We used this assay to carry out a genomewide RNAi screen, which will be described elsewhere (L.C. and N.C.F., unpublished data). RNAi of *rab5*, a gene required for phagocytosis of bacteria (Ramet et al., 2001), markedly reduced the ability of S2 cells to engulf apoptotic cells, thereby confirming a general role for *rab5* in phagocytosis (Figure 2C; compare Figures S2E and S2F). RNAi of one of the eight genes that falls into the *Df(3R)3-4* deficiency region of interest, namely *CG10233*, also led to a significant reduction in the efficiency of S2 cells to engulf apoptotic cells (compare Figures 2A and 2B; Figure 2C). RNAi of the other seven genes (listed in Figure 1H) did not affect phagocytosis (data not shown). Thus, *CG10233* is the

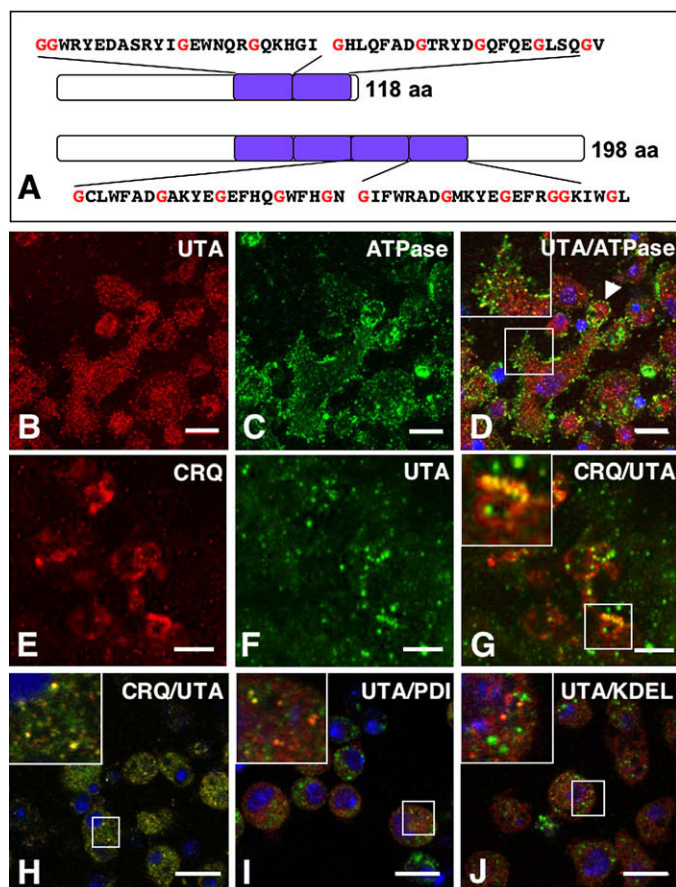


Figure 3. UTA Encodes a MORN Repeat-Containing Protein and Colocalizes with PM, ER, and Phagosomal Markers

(A) A schematic of the two isoforms encoded by *uta* with corresponding MORN repeat amino acid sequences.

(B–D) S2 cells costained with UTA (green) (B) and the Na⁺/K⁺ ATPase subunit (red) (C) Abs and the corresponding overlay (D), with DAPI in blue. (E–G) Embryonic macrophages costained with CRQ (red) (E) and UTA (green) (F) Abs and the corresponding overlay (G).

(H) S2 cells costained with both CRQ (green) and UTA (red) Abs, and DAPI (blue). Of note is that we could not distinguish the staining of UTA on the membrane of the apoptotic cell being engulfed from that of UTA on the phagosomal membrane of the engulfing cells.

(I and J) S2 cells costained with UTA (red) and PDI (green) Abs (I) or with UTA (red) and KDEL (green) Abs (J).

Scale bars in (B)–(D) and (H)–(J) represent 10 μm, and in (E)–(G) represent 5 μm.

predicted from its distribution, which is reminiscent of that of ER (Figure 3B), UTA colocalized with both PDI and KDEL in a subset of the ER (Figures 3I and 3J), supporting a role for UTA in coupling PM and ER in phagocytes.

The *Drosophila* Ryanodine receptor-encoding gene, *rya-r44F*, acts as a Ca²⁺ channel on the ER/SR membrane (Xu et al., 2000). *rya-r44F* mutants show slow feeding, locomotion, and heart rate that result in larval lethality (Sullivan et al., 2000), arguing that Rya-r44F plays a similar role to that of RyRs in mammals. To address whether Ca²⁺ release from the ER/SR storage compartment via Rya-r44F might play a role in phagocytosis of apoptotic cells, we used its specific antagonist, ryanodine. When treated with a 200 μM blocking concentration of ryanodine, the ability of S2 cells to engulf apoptotic cells was reduced by ~47% (Figure S3A). We assessed the phenotypes of two *rya-r44F* hypomorphic mutants, *rya-r44F¹⁶* and *rya-r44F^{K04913}* (Sullivan et al., 2000). As in *uta* deficiency embryos, *rya-r44F¹⁶* and *rya-r44F^{K04913}* homozygous macrophages were defective in phagocytosis of apoptotic cells (compare Figure 4A with Figures 4B and 4C), with PIs of 0.74 ± 0.34 and 0.72 ± 0.20, respectively (Figure 4D). Thus, *rya-r44F* is required for efficient phagocytosis, arguing that Ca²⁺ release from the ER/SR into the cytosol is integral to this process.

To address whether *uta* genetically interacted with *rya-r44F*, we assessed the phenotypes of embryos heterozygous for both the *uta* deficiency and either of the *rya-r44F* alleles.

Whereas single heterozygous macrophages had no phenotype, those in both double heterozygous combinations had a defect in apoptotic cell clearance, with PIs of 0.86 ± 0.21 and 0.79 ± 0.11 with *rya-r44F¹⁶* and *rya-r44F^{K04913}*, respectively (Figure 4D). These results argue that UTA acts together with Rya-r44F to promote efficient phagocytosis, and that UTA is likely to regulate Ca²⁺ homeostasis during this process by forming junctional complexes that link PM events to ER/SR Ca²⁺ release via Rya-r44F.

The release into the cytosol of Ca²⁺ from the ER/SR compartment promotes store-operated Ca²⁺ entry (SOCE) (Parekh and Putney, 2005). CRACM1/dOrai, a CRAC channel with similar properties to those in mammalian cells, was identified in genomewide RNAi screens for genes required for SOCE in S2 cells (Feske et al., 2006; Vig et al., 2006). *uta* was also found in one such SOCE RNAi screen (Vig et al., 2006). To confirm that *uta* plays a role in SOCE, we tested *uta* RNAi-treated S2 cells (knocked down by 61%; Table S1) for their ability to trigger SOCE after thapsigargin (TG) treatment, a binding inhibitor of the ER Ca²⁺ ATPase (SERCA) pump. TG treatment leads to net leakage of Ca²⁺ from the ER and a rise in intracellular Ca²⁺ concentration ([Ca²⁺]_i). This ER Ca²⁺ depletion leads to SOCE via CRAC channels in mock-treated S2 cells (Figure 4E). In the absence of TG, *uta* RNAi cells behaved like mock-treated cells and elicited a similar extracellular Ca²⁺ uptake via ER store-independent Ca²⁺ channels (Figure S5). Upon TG treatment, *uta* RNAi-treated S2 cells failed to elicit SOCE after 2 mM Ca²⁺ addition to the medium, as for *dorai* and *dstim* RNAi control cells (Figure 4E). We observed a range of responses to TG in *uta* RNAi-treated cells, with cells that were as efficient as mock-treated cells or weakly elicited ER Ca²⁺ release, all failing to trigger Ca²⁺ entry via dOrai (Figure S4). Although observing cells that weakly released Ca²⁺ from the ER after TG treatment was consistent with previous reports that JPs are required for the opening of the RyRs, mock-treated S2 cells showed a similar heterogeneity in response to TG as *uta* RNAi-treated cells (Figure S4). This might be due to the heterogeneity in population of S2 cells. Regardless, our average results (Figure 4D) agree with those obtained with mammalian cells, where JPs have been shown to be required for SOCE independently of ER Ca²⁺ release (Hirata et al., 2006), and support a similar role for

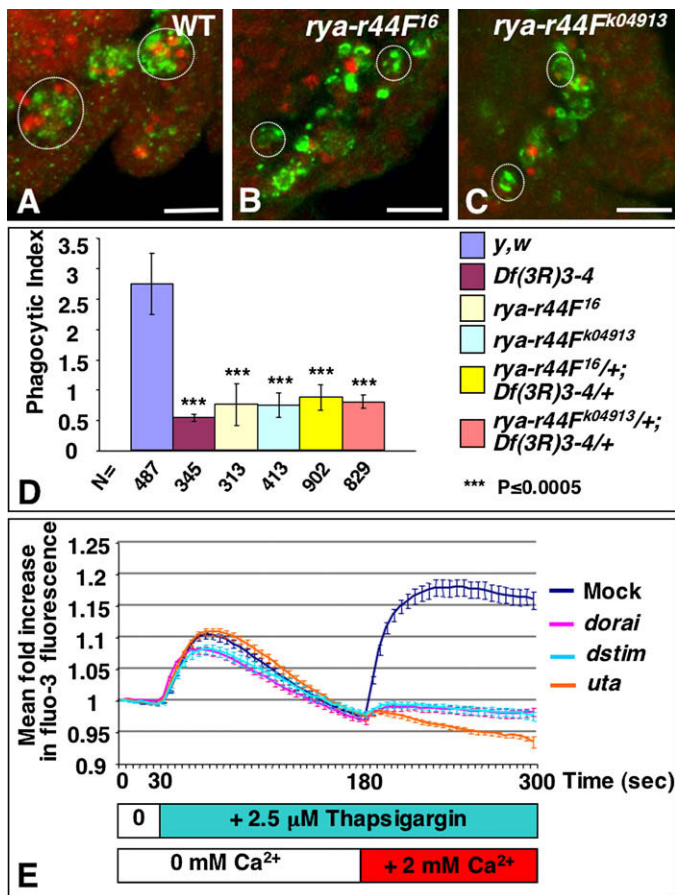


Figure 4. Requirement for the *Drosophila* Ryanodine Receptor-Encoding Gene, *rya-r44F*, which Genetically Interacts with *uta* (A–C) Macrophages of stage 13 wild-type (A), homozygous *rya-r44F*¹⁶ (B), and *rya-r44F*^{k04913} (C) embryos stained with the CRQ Ab (green) and apoptotic corpses detected with 7-AAD (red). Scale bars represent 10 μ m. (D) A graph of the corresponding PIs \pm SD, and of double heterozygous macrophages for the *uta* deficiency and each *rya-r44F* allele. (E) A graph of the changes in fluo-3AM fluorescence in mock, *dorai*, *dstim*, and *uta* RNAi-treated S2 cells exposed to 2.5 μ M TG in Ca²⁺-free medium at 30 s and to 2 mM extracellular Ca²⁺ 150 s later. Results are given as a fold increase of the mean fluo-3 fluorescence \pm SEM measured over time.

UTA in SOCE. They do not, however, support a role for UTA in ER Ca²⁺ release after TG treatment. By analogy with JPs and their distribution between the ER and PM, UTA might still play a role in linking PM events to ER Ca²⁺ release in vivo (a role which may be bypassed by TG treatment). Further studies will be required to address this.

Store-Operated Ca²⁺ Entry Is Required for Efficient Phagocytosis of Apoptotic Cells

Because *uta* and *rya-r44F* are both required for phagocytosis of apoptotic cells, we asked whether extracellular Ca²⁺ entry downstream of Rya-r44F opening was also required. We incubated S2 cells with FITC-labeled apoptotic S2 cells in the presence of EGTA, which depletes S2 cells of extracellular Ca²⁺. The EGTA treatment reduced the ability of S2 cells to phagocytose apoptotic corpses by ~59% (68% \pm 5% engulfing cells in control versus 28% \pm 2% in EGTA-treated cells; $p \leq 0.003$); their viability was unaffected as demonstrated by CTB staining (compare Figures 5A and 5B). These results support a role for extracellular Ca²⁺ entry in phagocytosis of apoptotic cells by S2 cells, possibly via CRAC channels.

In the presence of 1 μ M BTP-2, a potent inhibitor of the CRAC channel (Zitt et al., 2004), S2 cells poorly engulfed apoptotic cells (Figure S3A). dSTIM and dOrai are essential for SOCE in S2 cells (Feske et al., 2006; Roos et al., 2005; Vig et al., 2006). To address whether these genes were required for apoptotic cell clearance,

we knocked them down by RNAi in S2 cells and assessed their mRNA expression levels (Table S1) and associated phenotypes (Figures 5C–5E). As for *uta*, *dstim* and *dorai* RNAi-treated S2 cells poorly engulfed apoptotic cells (Figures 5C–5E). Although there are currently no mutants for *dstim*, there are two lethal recessive P element insertions within the *dorai* gene (also known as *olf186-F*) that might disrupt its function (Figure S6). Homozygous mutant macrophages for each allele, namely *olf186-F*^{K11505} and *olf186-F*^{EY09167}, were phagocytosis defective (compare Figures 5F and 5G; data not shown), with PIs of 0.75 \pm 0.08 and 0.67 \pm 0.04, respectively (Figure 5I). Moreover, each allele genetically interacted with the *uta* deficiency (Figures 5H and 5I; data not shown), with PIs of 0.67 \pm 0.14 and 0.73 \pm 0.17, for the respective double heterozygotes. Thus, *dstim* and *dorai* are required for phagocytosis of apoptotic cells in the same pathway as *uta* and *rya-r44F*.

To examine Ca²⁺ homeostasis in vivo, we expressed the Ca²⁺ reporter transgene *UAS::GCaMP1.6* under the control of *crq::Gal4* (Movies 1A and 1B). We observed highly dynamic fluctuations of intracellular Ca²⁺ levels, where increases in GCaMP fluorescence, reflecting increased levels of Ca²⁺, were observed in macrophages preceding apoptotic cell engulfment; a decrease in GCaMP fluorescence was observed once the particle was fully ingested (Movie 2). These results are consistent with a previous report showing a rise in [Ca²⁺]_i upon particle binding by neutrophils, which rapidly resolves to basal [Ca²⁺]_i after phagosome closure around the particle (Dewitt and Hallett, 2002).

UTA and Rya-r44F Link the DRPR/drCed-6 Pathway to Ca²⁺ Homeostasis during Phagocytosis

In *C. elegans*, the scavenger receptor-related CED-1 accumulates around apoptotic cells during engulfment; CED-6, an adaptor for CED-1, and CED-7, an ATP-binding cassette transporter, all act in the same phagocytic pathway (Mangahas and Zhou, 2005). The precise role of this pathway, however, is not well understood.

In our deficiency screen, we found that *Df(2R)w45-30n*, which, among other genes, deletes *drced-6*, was phagocytosis defective with a PI of 0.68 \pm 0.15 (Figure 6D). A P element insertion predicted to mutate *drced-6*, *drced-6*^{KG03411a}, was also defective (compare Figures 6A and 6B) with a PI of 0.78 \pm 0.21 (Figure 6D), confirming a previously reported role for *drced-6* in phagocytosis of apoptotic cells (Awasaki et al., 2006; Hoopfer et al., 2006).

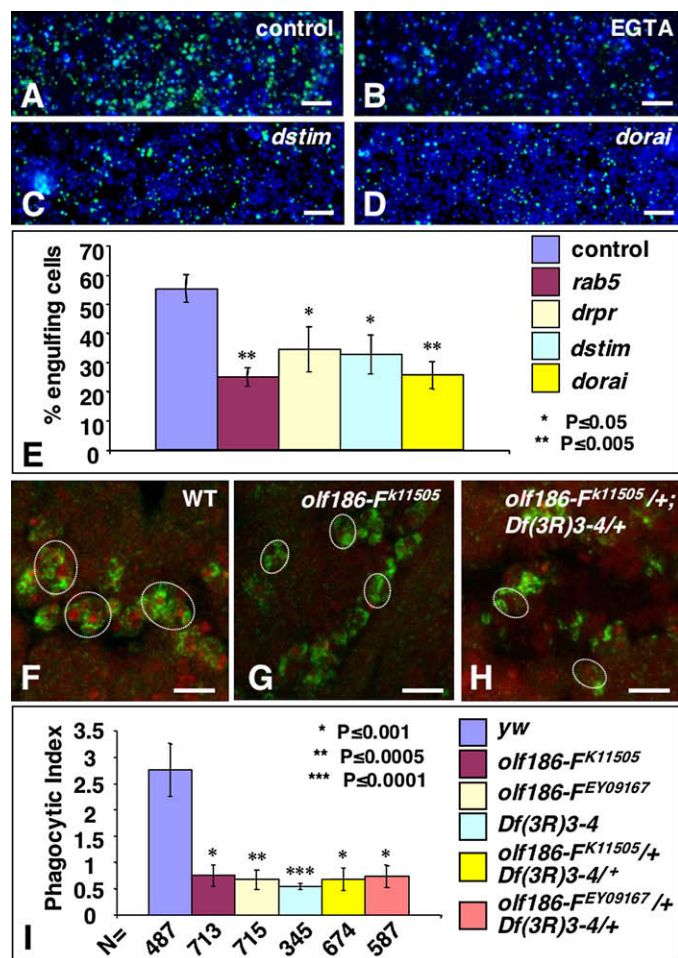


Figure 5. Requirement for SOCE in Phagocytosis of Apoptotic Cells

(A–D) Phagocytosis of apoptotic cells (green) by S2 cells (blue) in the absence (A) or presence (B) of 2 mM EGTA, or by *dstim* (C) and *dorai* (D) RNAi-treated S2 cells. Scale bars represent 200 μ m.

(E) A graph summarizing these assays, where bars represent the mean percentage of engulfing cells \pm SEM of three independent experiments in duplicates.

(F–H) Wild-type (F), *ora^{K11505}* homozygous mutant (G), and *ora^{K11505}/+*; *Df(3R)3-4/+* double heterozygous macrophages stained with CRQ Ab (green) and 7-AAD (red). Scale bars represent 10 μ m.

(I) A graph of the mean PIs \pm SD.

We confirmed that, as for *uta*, *dorai*, and *dstim*, *drced-6* was required for SOCE, as *drced-6* RNAi-treated S2 cells failed to elicit Ca^{2+} entry upon TG treatment (Figure 6E). Surprisingly, *drpr* RNAi-treated S2 cells also appeared less responsive to Ca^{2+} addition after TG treatment, arguing that *drpr* is also required for SOCE (Figure 6E). Neither *drced-6* nor *drpr* RNAi-treated S2 cells failed to trigger Ca^{2+} entry via ER store-independent Ca^{2+} channels in the absence of TG treatment, thus solely playing a role in SOCE (Figure S5). Thus, UTA, Rya-r44F, DRPR, and drCed-6 act in the same pathway that regulates Ca^{2+} homeostasis during phagocytosis of apoptotic cells.

Store-Operated Ca^{2+} Entry Is Required for Efficient Phagocytosis of Bacteria

In mammals, phagocytes engulfing various particles exhibit a rise in $[Ca^{2+}]_i$ (Dewitt and Hallett, 2002; Rubartelli et al., 1997; Tejle et al., 2002), arguing that SOCE is generally associated with phagocytosis. We asked whether *uta*, *dstim*, and *dorai* might be required for phagocytosis of Gram-negative or -positive bacteria by exposing RNAi-treated S2 cells to either *E. coli* or *S. aureus* labeled with pHrodo, a dye that fluoresces in the acidic environment of a mature phagosome upon fusion with lysosomes (Fiala et al., 2007). No fluorescence could be detected when the assay was performed at 26°C in the presence of cytochalasin D, or at 4°C, conditions where phagocytosis is prevented (Figures S7A–S7D; data not shown). As with apoptotic cells, *uta*, *dstim*, and *dorai* RNAi-treated S2 cells poorly phagocytosed *E. coli* and *S. aureus* (Figure 7A). Ryanodine and the CRAC channel inhibitor BTP-2 also inhibited bacterial engulfment (Figures S3B and S3C). These results demonstrate a role for SOCE in bacterial phagocytosis.

To examine Ca^{2+} changes in response to bacterial engulfment in vivo, we injected *UAS::GCaMP1.6* reporter-expressing embryos with TRITC-labeled *E. coli* (to visualize the red bacterium prior to and throughout engulfment). Correlating an increase in GCaMP fluorescence (i.e., Ca^{2+}) in macrophages upon particle binding in vivo is difficult, as macrophages may receive other stimuli affecting their $[Ca^{2+}]_i$ (such as an apoptotic stimulus). However, macrophages showed high GCaMP fluorescence (i.e., Ca^{2+} level) after bacterial injection. As seen in apoptotic cell engulfment, the macrophage GCaMP fluorescence (i.e., Ca^{2+} level) dropped following recognition of bacteria that appeared to have been taken up into a mature phagosome, as

Remarkably, as for *uta*, *drced-6* was also a hit in a genomewide RNAi screen for SOCE (Vig et al., 2006). Thus, we tested whether the *uta* deficiency and *drced-6^{KG03411a}* allele might genetically interact. We found that double heterozygous macrophages poorly engulfed apoptotic cells, with a PI of 0.78 ± 0.06 (Figure 6D). This phenotype was rescued by driving the *UAS::CG10233* (*uta*) transgene expression with *crq::Gal4* in the double heterozygous background (PI of 2.24 ± 0.24 ; $p = 0.1$) (Figure 6D). Heterozygous for *drced-6^{KG03411a}* and *Df(3R)ED5156*, which does not delete *uta*, were wild-type for phagocytosis (PI of 2.69 ± 0.39 ; $p = 0.91$).

Consistent with *drpr* being required for apoptotic cell clearance (Manaka et al., 2004), macrophages in homozygous embryos for the *drpr^{rec8.45}* null allele (Freeman et al., 2003) were phagocytosis defective, with a PI of 0.78 ± 0.06 (compare Figures 6A and 6C; see Figure 6D). Whereas macrophages in embryos heterozygous for *drpr^{rec8.45}*, and for *Df(3R)ED5156* and *drpr^{rec8.45}*, had a wild-type phenotype with PIs of 2.39 ± 0.40 ($p = 0.28$) and 2.53 ± 0.47 ($p = 0.54$), respectively, macrophages in embryos double heterozygous for *drpr^{rec8.45}* and the *uta* deletion, or for *drpr^{rec8.45}* and the *rya-r44^{K04913}* hypomorphic allele, were phagocytosis defective with PIs of 0.48 ± 0.15 and 0.68 ± 0.14 , respectively (Figure 6D). These results demonstrate a genetic link between *uta*, *rya-r44F*, and the *drpr/drced-6* pathway.

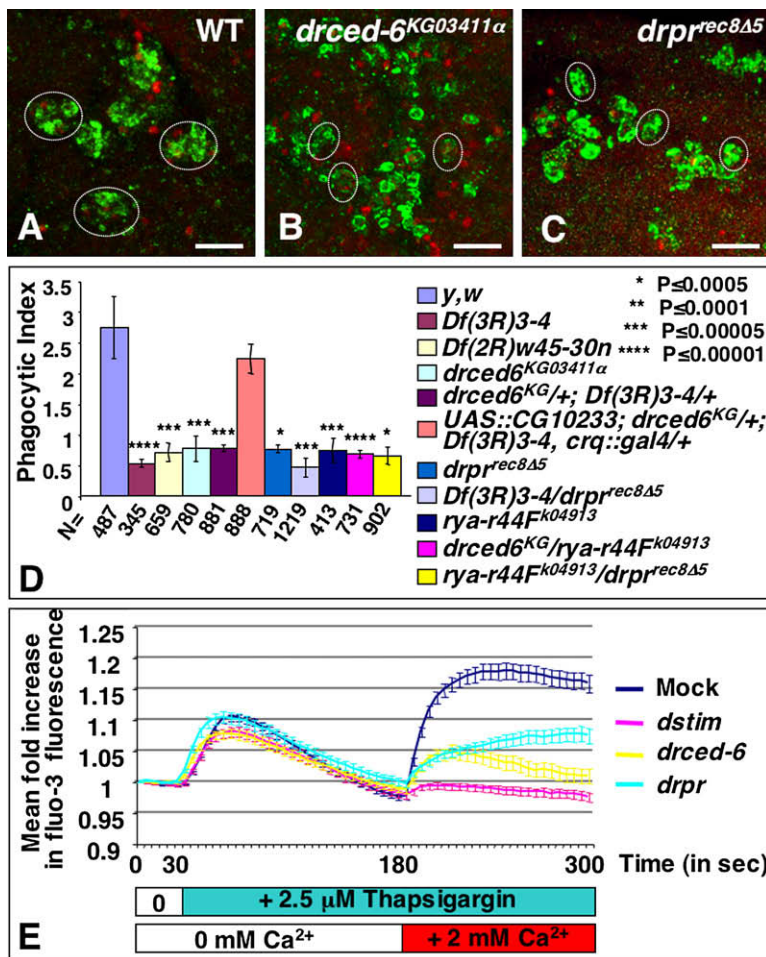


Figure 6. *drCed-6* and *drpr* Genetically Interact with *uta* and *rya-r44F* and Are Required for Phagocytosis and SOCE

(A–C) Macrophages of stage 13 wild-type (A), homozygous *dced6*^{KG03411a} (B), and *drpr*^{rec8Δ5} (C) mutant embryos immunostained with the CRQ Ab (green) and apoptotic corpses detected with 7-AAD (red). Scale bars represent 10 μm.

(D) A graph of the mean PIs ± SD for each double or trans-heterozygous combination compared to homozygous gene mutations.

(E) Changes in fluo-3AM fluorescence of mock, *dstim*, *drCed-6*, and *drpr* RNAi-treated cells. Results are given as a fold increase of the mean fluo-3 fluorescence ± SEM measured over time.

To assess whether bacterial engulfment may be less efficient in *drced-6*^{KG03411a} and *drpr*^{rec8Δ5} mutants, we injected pHrodo-labeled *E. coli* or *S. aureus* in homozygous adults (Figures 7C, 7D, 7F, and 7G). Preinjection of latex beads into adults saturated phagocytosis and prevented uptake of pHrodo bacteria in subsequent injections, and served as controls (compare Figures S6E and S6F). In *drced-6*^{KG03411a} and *drpr*^{rec8Δ5} mutant flies, macrophages poorly engulfed bacteria, as less fluorescence could be observed within their abdomens than in wild-type flies (compare Figures 7C and 7D with Figure 7B, and Figures 7F and 7G with Figure 7E). Thus, *uta*, *dstim*, *dorai*, *drced-6*, and *drpr* are all required for efficient clearance of apoptotic cells and bacteria, demonstrating a general role for SOCE in phagocytosis. This also provides evidence for a previously unappreciated role for the DRPR/drCed-6 pathway in bacterial engulfment, although additional studies will be required to assess its role in host defense upon bacterial infection.

suggested by their sustained discoloration from red to a slightly orange color (Movie 3).

DRPR and drCed-6 Play a Role in Bacterial Phagocytosis

A role for *drpr* and *drced-6* was previously described only in apoptotic cell clearance (Awasaki et al., 2006; MacDonald et al., 2006; Manaka et al., 2004). Our findings that *uta*, *dstim*, and *dorai* generally acted in phagocytosis and genetically interacted with *drced-6* and *drpr* suggested a possible role for these two genes also in bacterial engulfment. *drced-6* and *drpr* RNAi-treated S2 cells were indeed defective in bacterial phagocytosis (Figure 6E). This was not the result of a lack of specificity in our phagocytosis assays: *crq* RNAi-treated S2 cells failed to efficiently engulf apoptotic cells (Figure S3A), as well as *S. aureus* (Figure S3C), but engulfed *E. coli* as efficiently as mock-treated S2 cells (Figure S3B). These results are consistent with a known role for CRQ in phagocytosis of apoptotic cells (Franc et al., 1999) and of *S. aureus* (Stuart et al., 2005). As previously reported (Kocks et al., 2005), *eater* RNAi-treated cells failed to efficiently engulf both *E. coli* and *S. aureus*, but efficiently engulfed apoptotic cells (Figures S3A–S3C). These results highlight complexity in the molecular mechanisms underlying recognition specificity: neither CRQ nor DRPR appear to be uniquely involved in the recognition of apoptotic cells, or of Gram-positive or -negative bacteria.

DISCUSSION

Binding of various particles induces a rise in [Ca²⁺]_i in mammalian phagocytes (Dewitt and Hallett, 2002; Rubartelli et al., 1997; Tejle et al., 2002). In dendritic cells, [Ca²⁺]_i increases upon apoptotic cell binding via integrin, and inhibition studies have suggested that both Ca²⁺ release from the ER/SR storage pool and extracellular Ca²⁺ entry into the cytosol are required for this process (Rubartelli et al., 1997). Neutrophils also rely on such changes to promote particle engulfment (Dewitt and Hallett, 2002; Kindzelskii and Petty, 2003). Yet, the molecular mechanisms underlying this rise in [Ca²⁺]_i and what role it plays in phagocytes are poorly understood.

We found that *uta*, a *Drosophila* gene encoding a JP-related protein, is required for phagocytosis of apoptotic cells. We provided genetic evidence of a role for a Ryanodine receptor, *Rya-r44F*, and genetically linked *uta* and *rya-r44F*. We also found that SOCE via *dstim* and *dorai* promotes efficient apoptotic cell clearance. We genetically linked *uta* and *rya-r44F* to *drpr* and *drced-6*, and found a role for *uta*, *drpr*, and *drced-6* in SOCE, thus demonstrating a functional link between the DRPR/drCed-6 pathway and SOCE during phagocytosis.

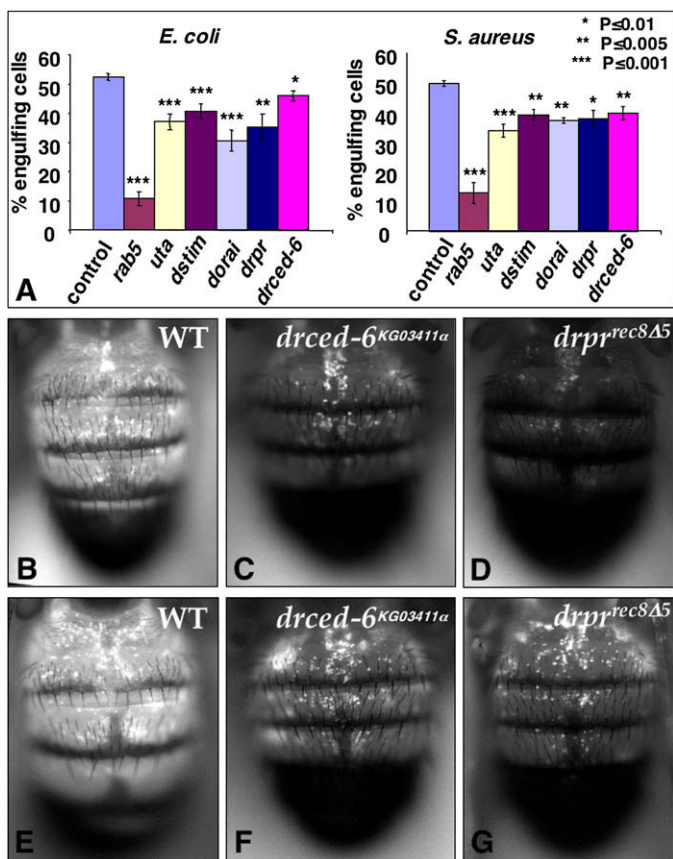


Figure 7. *drCed-6* and *drpr* Are Required for Bacterial Phagocytosis

(A) Graphs summarizing pHrodo *E. coli* or *S. aureus* engulfment by RNAi-treated cells for *uta*, *dstim*, *dorai*, *draper*, and *drCed-6*. Results are given as a percentage of engulfing cells \pm SEM.

(B–G) Abdomens of control *w* flies (B and E), and *drCed-6*^{KG03411a} (C and F) and *drpr*^{rec8Δ5} (D and G) homozygous mutant flies injected with pHrodo *E. coli* (B–D) or *S. aureus* (E–G). The bright white spots seen in the abdomen correspond to bacteria that were engulfed by plasmatocytes (adult macrophage-equivalent).

their downstream signaling cascade (Figure S8B). Although further studies will be required to test the validity of this proposal, several reports already support it: DRPR-mediated phagocytosis depends on Src and Syk family kinase signaling (Ziegenfuss et al., 2008), and the activity of such kinases can be Ca²⁺ dependent in mammalian cells (Papp et al., 2007; Wang et al., 1994).

We then proposed that signaling downstream of DRPR and *drCed-6* promotes and/or maintains the formation of UTA junctional complexes (Figure S8C), thereby linking ER Ca²⁺ release to SOCE (Figure S8D). dSTIM is indeed likely to act as an ER Ca²⁺ sensor that oligomerizes (Luik et al., 2008) and redistributes to ER-PM junctions upon ER Ca²⁺ depletion, as for its mammalian counterparts (Feske, 2007). We propose that UTA junctional complexes are needed to maintain a close proximity between the ER Ca²⁺ stores and the PM and to juxtapose dSTIM oligomers and dOrai, thereby promoting conformational changes and opening of dOrai (Figure S8D). DRPR- and *drCed-6*-dependent signaling and/or UTA may also be required for dSTIM oligomerization. The resulting increase in [Ca²⁺]_i then promotes engulfment of the particle.

Ca²⁺ may promote phagocytosis via several ways. It can enhance scavenger receptor (SR) activity: adhesion of mouse macrophages to a fibronectin-coated surface via integrin binding results in an increase in the number of SRs at their PM, which enhances their binding activity (Beppu et al., 2001). This enrichment in SRs is dependent on extracellular Ca²⁺ influx, arguing in favor of a role for Ca²⁺ in SR trafficking and/or recycling. Several SRs or related receptors play a role in phagocytosis of apoptotic corpses, including the mammalian CD36 (Savill et al., 1992) and its *Drosophila* homolog CRQ (Franc et al., 1999). Although we do not see a change in CRQ expression in *uta* mutant macrophages, CRQ and UTA colocalize and genetically interact (N.C.F., unpublished data). One possible model is that CRQ is recruited to the phagocytic cup upon apoptotic cell binding after SOCE that depends on UTA, DRPR, and *drCed-6*, and that this might strengthen the binding and uptake of the corpse.

In *C. elegans*, CED-1 (DRPR homolog) is related to the endothelial scavenger receptor SREC. Its recruitment to the phagocytic cup depends on functional CED-7 (Zhou et al., 2001), and may occur by exocytosis (Yu et al., 2006). Components of the exocyst were implicated in phagocytosis (Stuart et al., 2007). Moreover, Orai1 is required for degranulation of mast cells, which occurs by exocytosis (Vig et al., 2008). Thus, like Orai1, dOrai may be required for exocytosis and, whereas DRPR

We propose a model whereby apoptotic cell binding via DRPR (and possibly other receptors, such as CRQ) leads to ER Ca²⁺ release via Rya-r44F (Figure S8A). DRPR, which bears an immunoreceptor tyrosine-based activation motif (ITAM) that is phosphorylated via Src and Syk family kinase-mediated signaling, appears to behave like an immunoreceptor (Ziegenfuss et al., 2008). In B and T lymphocytes, engagement of Fc immunoreceptors (the signaling of which also relies on phosphorylation on ITAMs) leads to a rise in [Ca²⁺]_i (Feske, 2007). Thus, DRPR might play a similar role to that of Fc receptors in the signaling, leading to a rise in [Ca²⁺]_i in macrophages.

UTA is localized in the ER and at the PM. Thus, we propose that, like JPs, UTA forms junctional complexes that link the PM events to the ER and trigger Ca²⁺ release from ER stores (Figure S8A). Our studies, however, did not address whether the formation of UTA junctional complexes is required to trigger ER Ca²⁺ release via Rya-r44F, nor what triggers ER Ca²⁺ release. The resting membrane potential of mammalian phagocytes is depolarized upon contact with apoptotic cells (Vernon-Wilson et al., 2007). As in mammalian muscle cells, such changes in fly phagocytes might initiate ER Ca²⁺ release.

In S2 cells, our Ca²⁺ imaging results with *drpr* and *drced-6* RNAi (Figure 6E) and that of others with *drced-6* RNAi (Vig et al., 2006) suggest that *drpr* and *drced-6* are required for dOrai-mediated Ca²⁺ entry upon TG treatment (which bypasses the need for particle binding to the receptor). We propose that ER Ca²⁺ release feeds back onto DRPR and *drCed-6* to activate

appears to always be present at the PM (Freeman et al., 2003), CRQ may be recruited from its intracellular vesicular pool to the phagocytic cup by exocytosis, as previously proposed for CED-1, to promote apoptotic cell uptake.

A rise in Ca^{2+} was observed in mammalian neutrophils upon particle binding (Dewitt and Hallett, 2002), and Ca^{2+} participates in phagocytosis by promoting F-actin breakdown and phagosome maturation (Tejle et al., 2002). *Mycobacterium tuberculosis* is able to invade human macrophages without triggering an increase in $[Ca^{2+}]_i$: in the absence of Ca^{2+} signaling, phagosomes containing *M. tuberculosis* fail to mature, perhaps explaining the survival of this bacterium in the cell (Kusner, 2005). A role for Ca^{2+} in particle binding and phagosome maturation in macrophages, however, was once discounted (Zimmerli et al., 1996). *uta*, *dstim*, *dorai*, *drCed-6*, and *drpr* are required to trigger SOCE. Yet, although they are poorly phagocytic, macrophages in *drCed-6* hypomorphs and *drpr* null mutants engulf bacteria into fully matured phagosomes, arguing against Ca^{2+} being involved in phagosome maturation. This maturation, however, might still occur with lower efficiency when SOCE fails, as RNAi-treated S2 cells for all genes in this pathway poorly engulfed bacteria.

Our findings that UTA links DRPR-mediated phagocytosis and Ca^{2+} homeostasis provide us with the opportunity to pursue the dissection of the DRPR pathway in *Drosophila*. DRPR is homologous to CED-1, which belongs to the CED1/6/7 pathway where CED-7 is an ABC transporter. Interestingly, an ABC transporter can modulate Ca^{2+} channel activity in plants (Suh et al., 2007), further supporting a link between the CED1/6/7-like pathways and Ca^{2+} homeostasis, which appears to have been conserved throughout evolution. Furthermore, a mutation in human Orai1 was found in some patients with severe combined immune deficiency (Feske et al., 2006). Thus, pursuing such studies might be relevant to mammalian systems and to human health.

EXPERIMENTAL PROCEDURES

Fly Strains

Fly strains were from the Szeged or Bloomington *Drosophila* stock centers (unless otherwise specified) and crossed to a balancer chromosome carrying a *kr::GFP* transgene to select embryos of the appropriate genotype. We generated UAS transgenic flies following standard procedures by injecting a UAS construct and helper plasmid at the concentrations of 200 and 100 ng/ μ l, respectively. For in vivo rescue of *uta*, *crq::gal4* and *UAS::eGFP* were recombined onto the *Df(3R)3-4* chromosome to express cytoplasmic eGFP in macrophages specifically. *Df(3R)3-4*, *crq::gal4*, *UAS::eGFP* and *UAS::CG10233*; *Df(3R)3-4*, *crq::gal4*, *UAS::eGFP* homozygous embryos were identified based on dose-sensitive expression of GFP (Silva et al., 2007).

Acridine Orange, 7-AAD, Immunostainings, and Imaging

AO and 7-AAD stainings were performed as previously described (Silva et al., 2007). In immunostainings, the Abs used were rabbit anti-CRQ (1:1000), rat anti-CRQ (1:100), mouse anti-GFP (Roche; 1:4000), mouse anti-KDEL (Calbiochem; 1:200), mouse anti-PDI (Abcam; 1:250), rabbit anti-Retinophillin (1:100), and mouse anti- Na^+/K^+ ATPase (Developmental Studies Hybridoma Bank; 1:20), following standard methods. FITC-secondary Abs were from Vector Laboratories or Jackson Laboratories (1:1000); Cy5- and TRITC-coupled secondary Abs were from Jackson Laboratories (1:1,000). Nuclei of S2 cells were counterstained using DAPI-Vectashield (Vector Laboratories). Confocal imaging was performed on a Bio-Rad Radiance confocal microscope equipped with a Nikon upright microscope, or a Leica TCS SP5 confocal equipped with an inverted DMI6000 microscope.

Statistical Analyses of PIs

PIs were quantified as previously in Silva et al. (2007). Standard deviations (SD) were derived from the PIs calculated from four or five embryos per genotype. ANOVA tests comparing PIs between wild-type and mutants were calculated; p values are indicated in the figures.

Preparation of Apoptotic Cells

Exponentially grown S2 cells were treated with 0.25 μ g/ml of actinomycin D (Sigma) for 18 hr, fixed in 10% formaldehyde/serum-free Schneider medium (SFM), washed, and resuspended in 1 ml of SFM at a concentration equivalent to $8-10 \times 10^6$ cells/ml. Lyophilized FITC isomer (Molecular Probes) was resuspended to 100 μ l/ml in DMSO; 25 μ l was freshly added to 1 ml of apoptotic cells, incubated for 1 hr at room temperature, and washed twice in SFM.

Phagocytosis Assays

Exponentially growing S2 cells were plated at a density of $\sim 2.5-7.2 \times 10^3$ cells/ mm^2 . Apoptotic cells were added to live S2 cells at a ratio of 10:1; this ratio is a live cell to live cell ratio prior to apoptosis induction. Apart for the time course, cells were incubated for 5 hr or overnight, counterstained with 25 μ M Cell Tracker Blue CMAC (Molecular Probes) for 1 hr, and washed in PBS. Three hundred or 50 μ l of 0.4% trypan blue solution (Sigma) was added in a 24- or 384-well plate, respectively. Bacterial phagocytosis assays using pHrodo *E. coli* and *S. aureus* bioparticles (Invitrogen) were performed according to the manufacturer's instructions. Cells were treated with cytochalasin D at 10 μ M for 1 hr prior to adding particles.

RNA Interference

Amplicons were amplified from single-embryo DNA preparation as in Franc et al. (1999) or as described in Supplemental Experimental Procedures, where primer set (MWG Biotech AG) sequences are supplied. PCR cycles were as follows: 94°C for 3 min, followed by 94°C for 45 s, 57°C for 30 s, and 72°C for 45 s for 30 cycles, and a 10 min extension at 72°C. Double-stranded RNAs were produced using 1 μ g of amplicon and the T7 Megascript RNAi kit following Ambion's instructions. RNAi experiments were performed on exponentially growing cells, following the DRSC bathing protocol in either 384-well (for the screen), 96-well (for phagocytosis assays), or 6-well plates (for Ca^{2+} imaging) (<http://flymai.org/>). Engulfment assays were performed after 3 days, as described above.

Ca^{2+} Imaging

Cells were plated on a 32 mm glass bottom dish (Willco) and loaded with 2.5 μ M fluo-3 AM, a cell-permeant Ca^{2+} fluorophore, in 2 ml of complete medium with 6.25 mM probenidol for 45 min. Cells were washed twice with Ca^{2+} -free saline solution (120 mM NaCl, 5 mM KCl, 8 mM $MgCl_2$, 32.2 mM sucrose, 0.1 mM EGTA, 10 mM HEPES [pH 7.2]) with probenidol, and covered with 1.6 ml of this solution. Sixty time points were recorded with a lapse of 5 s between frames. TG ([2.5 μ M] final in Ca^{2+} -free solution) was added at 30 s; $CaCl_2$ was added at a final concentration of 2 mM, 150 s later. Images were analyzed using Volocity 4.2.0 (Improvision) by measuring the fluo-3 AM fluorescence of individual cells responding to TG over time. Mean values obtained for these cells from at least three independent experiments were calculated and the corresponding fold increases in fluorescence were derived, which are reported with corresponding standard errors from the mean (SEM).

Bacteria Injection Assay in Adult Flies

pHrodo *E. coli* and *S. aureus* bioparticles (Invitrogen) were resuspended according to the manufacturer's instructions, and 138 nl was injected into adult males using a Drummond Scientific Nanoject II. After 2 hr, the flies were mounted and imaged on an Axioskop Zeiss microscope with a Jenoptik/Jena ProgRes C14 camera.

SUPPLEMENTAL DATA

Supplemental Data include Supplemental Experimental Procedures, eight figures, one table, and four movies and can be found with this article online at [http://www.cell.com/supplemental/S0092-8674\(08\)01114-8](http://www.cell.com/supplemental/S0092-8674(08)01114-8).

ACKNOWLEDGMENTS

We thank the Bloomington and Szeged *Drosophila* stock centers, H. Agaisse, D. Ferrandon, M. Freeman, C. Kocks, B. Lemaitre, K. Mecklenberg, Y. Nakai, Y. Nakanishi, N. Perrimon, A. Rao, and D. Reiff for fly stocks and/or reagents and technical advice; A.V. for his help with Ca²⁺ imaging, and M. Hallett for his advice on its analysis; V. Keasler and W. Yu for the qPCR; H. Agaisse and members of the DRSC for their help with the RNAi screen, and members of the core staff for their help. N.C.F. thanks S. Brown, C. Desplan, and M. Meister for their critical reading of this manuscript. This research was funded by a programme leader-track grant from the Medical Research Council to N.C.F., core support to the MRC Cell Biology Unit, and a studentship from The Genetic Society UK to M.Q.

Received: February 26, 2008

Revised: May 28, 2008

Accepted: August 19, 2008

Published: October 30, 2008

REFERENCES

- Aderem, A., and Underhill, D.M. (1999). Mechanisms of phagocytosis in macrophages. *Annu. Rev. Immunol.* **17**, 593–623.
- Awasaki, T., Tatsumi, R., Takahashi, K., Arai, K., Nakanishi, Y., Ueda, R., and Ito, K. (2006). Essential role of the apoptotic cell engulfment genes *draper* and *ced-6* in programmed axon pruning during *Drosophila* metamorphosis. *Neuron* **50**, 855–867.
- Beppu, M., Hora, M., Watanabe, T., Watanabe, M., Kawachi, H., Mishima, E., Makino, M., and Kikugawa, K. (2001). Substrate-bound fibronectin enhances scavenger receptor activity of macrophages by calcium signaling. *Arch. Biochem. Biophys.* **390**, 243–252.
- Burlak, C., Whitney, A.R., Mead, D.J., Hackstadt, T., and Deleo, F.R. (2006). Maturation of human neutrophil phagosomes includes incorporation of molecular chaperones and endoplasmic reticulum quality control machinery. *Mol. Cell. Proteomics* **5**, 620–634.
- Dewitt, S., and Hallett, M.B. (2002). Cytosolic free Ca(2+) changes and calpain activation are required for β integrin-accelerated phagocytosis by human neutrophils. *J. Cell Biol.* **159**, 181–189.
- Feske, S. (2007). Calcium signalling in lymphocyte activation and disease. *Nat. Rev. Immunol.* **7**, 690–702.
- Feske, S., Gwack, Y., Prakriya, M., Srikanth, S., Puppel, S.H., Tanasa, B., Hogan, P.G., Lewis, R.S., Daly, M., and Rao, A. (2006). A mutation in *Orai1* causes immune deficiency by abrogating CRAC channel function. *Nature* **441**, 179–185.
- Fiala, M., Liu, P.T., Espinosa-Jeffrey, A., Rosenthal, M.J., Bernard, G., Ringman, J.M., Sayre, J., Zhang, L., Zaghi, J., Dejbakhsh, S., et al. (2007). Innate immunity and transcription of MGAT-III and Toll-like receptors in Alzheimer's disease patients are improved by bisdemethoxycurcumin. *Proc. Natl. Acad. Sci. USA* **104**, 12849–12854.
- Franc, N.C., Heitzler, P., Ezekowitz, R.A., and White, K. (1999). Requirement for croquemort in phagocytosis of apoptotic cells in *Drosophila*. *Science* **284**, 1991–1994.
- Freeman, M.R., Delrow, J., Kim, J., Johnson, E., and Doe, C.Q. (2003). Unwrapping glial biology: *Gcm* target genes regulating glial development, diversification, and function. *Neuron* **38**, 567–580.
- Hirata, Y., Brotto, M., Weisleder, N., Chu, Y., Lin, P., Zhao, X., Thornton, A., Komazaki, S., Takeshima, H., Ma, J., et al. (2006). Uncoupling store-operated Ca²⁺ entry and altered Ca²⁺ release from sarcoplasmic reticulum through silencing of junctophilin genes. *Biophys. J.* **90**, 4418–4427.
- Hoopfer, E.D., McLaughlin, T., Watts, R.J., Schuldiner, O., O'Leary, D.D., and Luo, L. (2006). Wlds protection distinguishes axon degeneration following injury from naturally occurring developmental pruning. *Neuron* **50**, 883–895.
- Kindzelskii, A.L., and Petty, H.R. (2003). Intracellular calcium waves accompany neutrophil polarization, formylmethionyleucylphenylalanine stimulation, and phagocytosis: a high speed microscopy study. *J. Immunol.* **170**, 64–72.
- Kocks, C., Cho, J.H., Nehme, N., Ulvila, J., Pearson, A.M., Meister, M., Strom, C., Conto, S.L., Hetru, C., Stuart, L.M., et al. (2005). Eater, a transmembrane protein mediating phagocytosis of bacterial pathogens in *Drosophila*. *Cell* **123**, 335–346.
- Kusner, D.J. (2005). Mechanisms of mycobacterial persistence in tuberculosis. *Clin. Immunol.* **114**, 239–247.
- Lebovitz, R.M., Takeyasu, K., and Fambrough, D.M. (1989). Molecular characterization and expression of the (Na⁺ + K⁺)-ATPase α -subunit in *Drosophila melanogaster*. *EMBO J.* **8**, 193–202.
- Lee, H.K., and Iwasaki, A. (2007). Innate control of adaptive immunity: dendritic cells and beyond. *Semin. Immunol.* **19**, 48–55.
- Luik, R.M., Wang, B., Prakriya, M., Wu, M.M., and Lewis, R.S. (2008). Oligomerization of STIM1 couples ER calcium depletion to CRAC channel activation. *Nature* **454**, 538–542.
- MacDonald, J.M., Beach, M.G., Porpiglia, E., Sheehan, A.E., Watts, R.J., and Freeman, M.R. (2006). The *Drosophila* cell corpse engulfment receptor *Draper* mediates glial clearance of severed axons. *Neuron* **50**, 869–881.
- Manaka, J., Kurashiki, T., Shiratsuchi, A., Nakai, Y., Higashida, H., Henson, P., and Nakanishi, Y. (2004). *Draper*-mediated and phosphatidylinositol-independent phagocytosis of apoptotic cells by *Drosophila* hemocytes/macrophages. *J. Biol. Chem.* **279**, 48466–48476.
- Mangahas, P.M., and Zhou, Z. (2005). Clearance of apoptotic cells in *Caenorhabditis elegans*. *Semin. Cell Dev. Biol.* **16**, 295–306.
- Mecklenburg, K.L. (2007). *Drosophila* retinophilin contains MORN repeats and is conserved in humans. *Mol. Genet. Genomics* **277**, 481–489.
- Papp, S., Fadel, M.P., Kim, H., McCulloch, C.A., and Opas, M. (2007). Calreticulin affects fibronectin-based cell-substratum adhesion via the regulation of c-Src activity. *J. Biol. Chem.* **282**, 16585–16598.
- Parekh, A.B., and Putney, J.W., Jr. (2005). Store-operated calcium channels. *Physiol. Rev.* **85**, 757–810.
- Pinto, M.P., Grou, C.P., Alencastre, I.S., Oliveira, M.E., Sa-Miranda, C., Franzen, M., and Azevedo, J.E. (2006). The import competence of a peroxisomal membrane protein is determined by Pex19p before the docking step. *J. Biol. Chem.* **281**, 34492–34502.
- Ramet, M., Pearson, A., Manfruelli, P., Li, X., Koziel, H., Gobel, V., Chung, E., Krieger, M., and Ezekowitz, R.A. (2001). *Drosophila* scavenger receptor *Cl* is a pattern recognition receptor for bacteria. *Immunity* **15**, 1027–1038.
- Roos, J., DiGregorio, P.J., Yeromin, A.V., Ohlsen, K., Lioudyno, M., Zhang, S., Saffrina, O., Kozak, J.A., Wagner, S.L., Cahalan, M.D., et al. (2005). STIM1, an essential and conserved component of store-operated Ca²⁺ channel function. *J. Cell Biol.* **169**, 435–445.
- Rubartelli, A., Poggi, A., and Zocchi, M.R. (1997). The selective engulfment of apoptotic bodies by dendritic cells is mediated by the $\alpha(v)\beta3$ integrin and requires intracellular and extracellular calcium. *Eur. J. Immunol.* **27**, 1893–1900.
- Ryder, E., Blows, F., Ashburner, M., Bautista-Llacer, R., Coulson, D., Drummond, J., Webster, J., Gubb, D., Gunton, N., Johnson, G., et al. (2004). The *DrosDel* collection: a set of P-element insertions for generating custom chromosomal aberrations in *Drosophila melanogaster*. *Genetics* **167**, 797–813.
- Savill, J., Hogg, N., Ren, Y., and Haslett, C. (1992). Thrombospondin cooperates with CD36 and the vitronectin receptor in macrophage recognition of neutrophils undergoing apoptosis. *J. Clin. Invest.* **90**, 1513–1522.
- Silva, E., Au-Yeung, H.W., Van Goethem, E., Burden, J., and Franc, N.C. (2007). Requirement for a *Drosophila* E3-ubiquitin ligase in phagocytosis of apoptotic cells. *Immunity* **27**, 585–596.
- Stuart, L.M., Deng, J., Silver, J.M., Takahashi, K., Tseng, A.A., Hennessy, E.J., Ezekowitz, R.A., and Moore, K.J. (2005). Response to *Staphylococcus aureus* requires CD36-mediated phagocytosis triggered by the COOH-terminal cytoplasmic domain. *J. Cell Biol.* **170**, 477–485.

- Stuart, L.M., Boulais, J., Charriere, G.M., Hennessy, E.J., Brunet, S., Jutras, I., Goyette, G., Rondeau, C., Letarte, S., Huang, H., et al. (2007). A systems biology analysis of the *Drosophila* phagosome. *Nature* **445**, 95–101.
- Suh, S.J., Wang, Y.F., Frelet, A., Leonhardt, N., Klein, M., Forestier, C., Mueller-Roeber, B., Cho, M.H., Martinoia, E., and Schroeder, J.I. (2007). The ATP binding cassette transporter AtMRP5 modulates anion and calcium channel activities in *Arabidopsis* guard cells. *J. Biol. Chem.* **282**, 1916–1924.
- Sullivan, K.M., Scott, K., Zuker, C.S., and Rubin, G.M. (2000). The ryanodine receptor is essential for larval development in *Drosophila melanogaster*. *Proc. Natl. Acad. Sci. USA* **97**, 5942–5947.
- Takekuma, H., Komazaki, S., Nishi, M., Iino, M., and Kangawa, K. (2000). Junctophilins: a novel family of junctional membrane complex proteins. *Mol. Cell* **6**, 11–22.
- Tejle, K., Magnusson, K.E., and Rasmusson, B. (2002). Phagocytosis and phagosome maturation are regulated by calcium in J774 macrophages interacting with unopsonized prey. *Biosci. Rep.* **22**, 529–540.
- Vernon-Wilson, E.F., Aurade, F., Tian, L., Rowe, I.C., Shipston, M.J., Savill, J., and Brown, S.B. (2007). CD31 delays phagocyte membrane repolarization to promote efficient binding of apoptotic cells. *J. Leukoc. Biol.* **82**, 1278–1288.
- Vig, M., Peinelt, C., Beck, A., Koomoa, D.L., Rabah, D., Koblan-Huberson, M., Kraft, S., Turner, H., Fleig, A., Penner, R., and Kinet, J.P. (2006). CRACM1 is a plasma membrane protein essential for store-operated Ca^{2+} entry. *Science* **312**, 1220–1223.
- Vig, M., DeHaven, W.I., Bird, G.S., Billingsley, J.M., Wang, H., Rao, P.E., Hutchings, A.B., Jouvin, M.H., Putney, J.W., and Kinet, J.P. (2008). Defective mast cell effector functions in mice lacking the CRACM1 pore subunit of store-operated calcium release-activated calcium channels. *Nat. Immunol.* **9**, 89–96.
- Wang, X., Sada, K., Yanagi, S., Yang, C., Rezaul, K., and Yamamura, H. (1994). Intracellular calcium dependent activation of p72syk in platelets. *J. Biochem.* **116**, 858–861.
- Xu, X., Bhat, M.B., Nishi, M., Takeshima, H., and Ma, J. (2000). Molecular cloning of cDNA encoding a *Drosophila* ryanodine receptor and functional studies of the carboxyl-terminal calcium release channel. *Biophys. J.* **78**, 1270–1281.
- Yu, X., Odera, S., Chuang, C.H., Lu, N., and Zhou, Z. (2006). *C. elegans* Dynamin mediates the signaling of phagocytic receptor CED-1 for the engulfment and degradation of apoptotic cells. *Dev. Cell* **10**, 743–757.
- Zhou, Z., Hartweg, E., and Horvitz, H.R. (2001). CED-1 is a transmembrane receptor that mediates cell corpse engulfment in *C. elegans*. *Cell* **104**, 43–56.
- Ziegenfuss, J.S., Biswas, R., Avery, M.A., Hong, K., Sheehan, A.E., Yeung, Y.G., Stanley, E.R., and Freeman, M.R. (2008). Draper-dependent glial phagocytic activity is mediated by Src and Syk family kinase signalling. *Nature* **453**, 935–939.
- Zimmerli, S., Majeed, M., Gustavsson, M., Stendahl, O., Sanan, D.A., and Ernst, J.D. (1996). Phagosome-lysosome fusion is a calcium-independent event in macrophages. *J. Cell Biol.* **132**, 49–61.
- Zitt, C., Strauss, B., Schwarz, E.C., Spaeth, N., Rast, G., Hatzelmann, A., and Hoth, M. (2004). Potent inhibition of Ca^{2+} release-activated Ca^{2+} channels and T-lymphocyte activation by the pyrazole derivative BTP2. *J. Biol. Chem.* **279**, 12427–12437.